JACS
JOURNAL OF THE AMERICAN CHEMICAL SOCIETY
Article
pubs.acs.org/JACS

Covalently Functionalized Double-Walled Carbon Nanotubes Combine High Sensitivity and Selectivity in the Electrical Detection of Small Molecules

Jia Huang,[†,#] Allen L. Ng,[†] Yanmei Piao,[†] Chien-Fu Chen,[†,‡] Alexander A. Green,[§] Chuan-Fu Sun,[†] Mark C. Hersam,[§] Cheng S. Lee,[†] and YuHuang Wang[†,∥,*]

[†]Department of Chemistry and Biochemistry, University of Maryland, College Park, Maryland 20742, United States

[‡]Graduate Institute of Biomedical Engineering, National Chung Hsing University, Taichung, Taiwan

[§]Department of Materials Science and Engineering and Department of Chemistry, Northwestern University, Evanston, Illinois, 60208-3108, United States

[∥]Maryland NanoCenter, University of Maryland, College Park, Maryland 20742, United States

Supporting Information

ABSTRACT: Atom-thick materials such as single-walled carbon nanotubes (SWCNTs) and graphene exhibit ultrahigh sensitivity to chemical perturbation partly because all of the constituent atoms are surface atoms. However, low selectivity due to nonspecific binding on the graphitic surface is a challenging issue to many applications including chemical sensing. Here, we demonstrated simultaneous attainment of high sensitivity and selectivity in thin-film field effect transistors (TFTs) based on outer-wall selectively functionalized double-walled carbon nanotubes (DWCNTs). With carboxylic acid functionalized DWCNT TFTs, we obtained excellent gate modulation (on/off ratio as high as 4000) with relatively high ON currents at a CNT areal density as low as 35 ng/cm^2. The devices displayed an NH_3 sensitivity of 60 nM (or ~1 ppb), which is comparable to small molecule aqueous solution detection using state-of-the-art SWCNT TFT sensors while concomitantly achieving 6000 times higher chemical selectivity toward a variety of amine-containing analyte molecules over that of other small molecules. These results highlight the potential of using covalently functionalized double-walled carbon nanotubes for simultaneous ultrahigh selective and sensitive detection of chemicals and illustrate some of the structural advantages of this double-wall materials strategy to nanoelectronics.

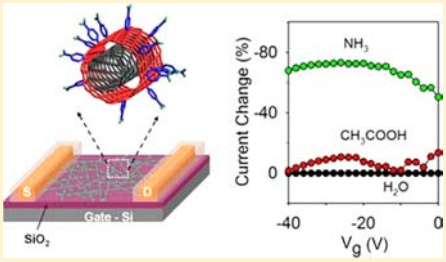

INTRODUCTION

One of the major challenges and opportunities in nanoscience lies in developing the ability to utilize the exceptional electrical properties of nanomaterials in complex chemical environments such as solar cells, fuel cells, microprocessors, and sensors. In the context of a sensor application, there is hope that nanomaterials will allow for fabrication of electrical sensors capable of detecting ultralow concentrations of analytes, e.g., explosives (such as TNT, nitroglycerin, cyclotetramethylene-tetranitramine) and biomolecules (such as HIV), with ultrahigh selectivity such that trace interferents will not trigger false positives. Various nanostructures and strategies have been explored for meeting this challenge. Some of the most sensitive sensors are based on graphene and pristine single-walled carbon nanotubes (SWCNTs).[1−13] In several specific cases, some success has also been achieved with noncovalent functionalization of the surface with receptor molecules to overcome nonspecific binding.[2,14,15] However, low long-term stability and incomplete surface coverage of noncovalent coatings remain general concerns for more demanding applications such as in vivo studies and those involving more aggressive chemical reactions that require a more stable and robust platform.[16] Covalent attachment of receptor molecules to the surface is an effective strategy for improving chemical selectivity. However, the number of functional groups that can be covalently attached to a SWCNT sidewall or graphene surface is extremely limited since covalent modifications quickly destroy their electrical properties.[17]

Here, we demonstrate simultaneous high sensitivity and chemical selectivity in covalently functionalized DWCNT (*f*-DWCNT) thin film transistors (TFTs) (Figure 1). A DWCNT consists of two concentric SWCNTs that exhibit complicated but relatively independent electronic properties.[18] Field-effect transistors integrating individual, pristine DWCNTs have been shown to have high on/off ratios (>10^3) and exceptional conductivity,[19,20] which are desirable for many electronics applications such as sensors. Advances in synthesis[21,22] and purification of DWCNTs[23,24] have made it possible to fabricate high quality thin film devices. Particularly, recent experiments by our group[25,26] and others[20] have shown that the electrical properties of inner tubes can be retained even after heavy

Received: November 5, 2012
Published: January 17, 2013

 © 2013 American Chemical Society dx.doi.org/10.1021/ja310844u | *J. Am. Chem. Soc.* 2013, 135, 2306−2312

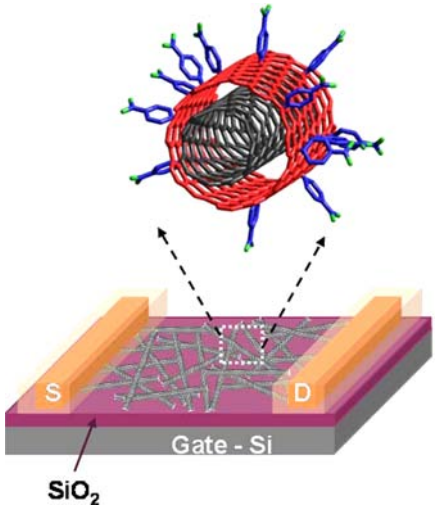

Figure 1. Schematic diagram of a *f*-DWCNT TFT platform that combines semiconducting inner tubes as transducer elements and chemically tailored outer walls for improved chemical selectivity.

functionalization of the outer wall by covalent chemistries. Furthermore, changes to the chemical or electrochemical environment at the surface of the outer wall of a DWCNT have been shown to induce electrical changes to the inner-wall of a DWCNT, suggesting the possibility of sensitive chemical detection via charge transport through the well-defined and chemically protected inner-wall.[27,28] In this report, we heavily functionalized the outer wall of the DWCNTs using diazonium chemistry, which readily provides a variety of terminating groups, including −COOH, −OH, $-CH_3$, $-NO_2$.[29,30] Because the inner tubes are hermetically sealed by the functional outer wall, nonspecific binding can be significantly reduced. We found that the transduction performance of the inner tube can be superior to other structures such as embedding SWCNTs in a functional coating or functionalized silicon nanowires, since the functionalized outer wall provides complete surface coverage and is only one atom-thick. This double-wall structure thus makes it possible to fabricate high performance chemical sensors with tailored surface chemistry to simultaneously achieve ultrahigh sensitivity and selectivity along with long-term stability.

RESULTS AND DISCUSSION

As a demonstration and proof of concept, we fabricated DWCNT TFTs from high-purity DWCNTs[23] and compared their device performance with SWCNTs and multiwalled carbon nanotubes (MWCNTs). The DWCNT TFT devices were covalently functionalized with $-C_6H_4COOH$ functional groups by reacting with 4-carboxylbenzenediazonium tetrafluoroborate in the dark at room temperature. Successful covalent functionalization of the outer wall was confirmed by comparative Raman spectroscopy studies of DWCNTs and SWCNTs before and after the functionalization (Figure 2 and Supporting Information, SI, Figure S2). After functionalization, the disorder mode (D band) around 1310 cm^{-1} appeared, signifying covalent modification of the nanotube sidewalls. In the functionalized DWCNTs, the radial breathing mode (RBM) of the inner tube (200−400 cm^{-1}) remained intact while that of the outer wall (under 200 cm^{-1}) completely disappeared, unambiguously confirming selective covalent functionalization of the outer wall. We note an increase in

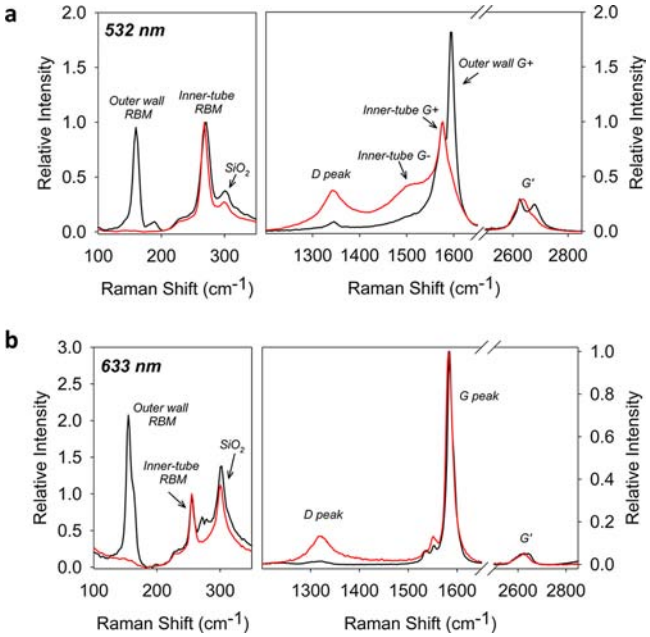

Figure 2. Raman spectra of DWCNT thin films before (black line) and after covalent functionalization with $-C_6H_4COOH$ groups (red line) for excitation lines of (a) 532 nm and (b) 633 nm showing evidence of outer wall selective covalent functionalization.

the G^- mode of inner tubes after functionalization, whose origin is not clear but may be due to a weakened wall-to-wall interaction due to outer wall functionalization.

Figure 3 shows the *I*−*V* characteristics of the p-type DWCNT TFTs (Figure 3a,b) in comparison with similarly fabricated p-type SWCNT TFTs and MWCNT TFTs before and after covalent surface modification with $-C_6H_4COOH$ functional groups. After heavy covalent functionalization, the SWCNT TFT device lost all of its electrical conductivity and transistor characteristics (Figure 3e,f). In contrast, MWCNTs did not show a significant decrease in electrical conductivity, but the highly metallic nature of the MWCNTs resulted in very low on/off ratios (∼1). These MWCNT TFTs, with and without functionalization, exhibit characteristics of resistors rather than that of transistors as evident by their negligible gate amplification effects (Figure 3h,i); for sensing purposes, it is more desirable to have transistor properties especially a high on/off ratio which allows for gate modulation and amplification of drain current response. For DWCNT TFTs, pristine devices exhibited modest on-current with relatively high on/off ratios. After covalent functionalization, the devices showed 5−10 times lower source-drain current; the source-drain current at V_g= −40 V and V_{SD}= −1 V was reduced from 5.5 to 1.2 μA. However, the source-drain current of covalently functionalized DWCNT TFTs was still on the same magnitude of pristine SWCNTs and their transistor characteristics, most importantly, were retained (Figure 3b,c). Table 1 compares the on-current, on/off ratio, and chemical selectivity of SWCNT, DWCNT, and MWCNT TFTs before and after covalent functionalization. These results confirm that inner tubes in the covalently functionalized double-wall structure uniquely possess desirable semiconductor characteristics.

Upon exposure to analytes, a p-type CNT TFT with a high on/off ratio has an enhanced response when the device is turned on by applying a negative gate voltage. This phenomena arises because semiconducting CNTs are typically more

dx.doi.org/10.1021/ja310844u | *J. Am. Chem. Soc.* 2013, 135, 2306−2312

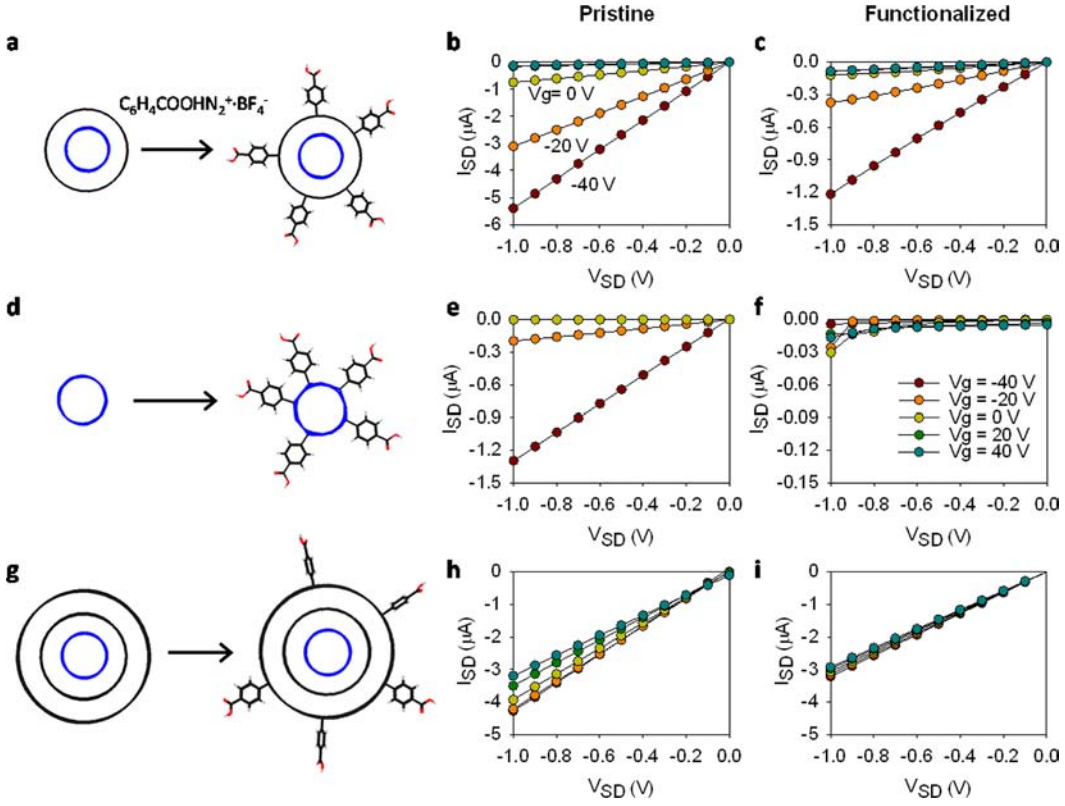

Figure 3. Source-drain $I-V$ curves of *f*-DWCNT TFTs show persistent transistor properties in stark contrast to their single-walled and multiwalled counterparts.

Table 1. Chemical sensing characteristics of covalently functionalized DWCNT TFTs in comparison towards other pristine and functionalized CNT TFTs

		on current	on/off ratio	selectivity
SWCNT	pristine	high	high	low
	functionalized	low	N/A	N/A
DWCNT	pristine	high	high	low
	functionalized	high	high	high
MWCNT	pristine	high	low	low
	functionalized	high	low	low

sensitive to analytes than metallic CNTs.[11] When the TFT is turned on by applying a negative gate voltage, the semiconducting CNTs become conductive. When a high positive gate voltage is applied, the TFT is turned off and the semiconducting CNTs are insulating. A high on/off ratio is indicative of a large ratio of semiconducting CNTs to metallic CNTs in the conduction channel. In this scenario, semiconducting CNTs contribute to the majority of the drain current when the CNT TFT is turned on. Those semiconducting CNTs at the "ON" stage are sensitive to analytes due to charge transfer or trapping effects. The gate modulation effect can thus amplify the responsive component of the drain current and increase sensor response. Figure S3 of the SI shows the normalized gate-dependent response of a functionalized DWCNT TFT upon exposure to 60 μM NH_3 as a function of gate voltage. At a V_g of −40 V, the TFT was turned on and about 70% current reduction was observed when the device was exposed to NH_3 solution. When the TFT was turned off at a V_g of +40 V, only about 5% current response was observed, illustrating that semiconducting DWCNTs are more responsive to analytes than metallic DWCNTs and the importance of gate amplification effects in a DWCNT TFT sensor.

The electrical characteristics of DWCNT TFTs highly depend on the areal density of DWCNTs in the conduction channel, which can be straightforwardly controlled by adjusting the volume and concentration of the DWCNT solution used for filtration. Figure 4 shows the source-drain current and on/off ratio of DWCNT thin-film TFTs as a function of DWCNT areal density. For each areal density, five devices were fabricated and measured. The DWCNT areal density was calculated by dividing the mass of DWCNTs in the solution by the filtration membrane area.

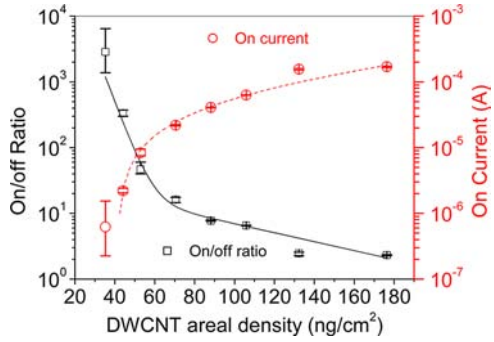

Figure 4. High source-drain current and on/off ratio can be simultaneously achieved in DWCNT TFTs at a network density around 50 ng/cm^2. The source-drain current at V_g = −40 V and V_{SD} = −1 V (red) and on/off ratio (black) of DWCNT TFTs were plotted as a function of DWCNT areal densities.

dx.doi.org/10.1021/ja310844u | *J. Am. Chem. Soc.* 2013, 135, 2306−2312

We found that both high on/off ratio and ON current can be simultaneously achieved at DWCNT densities around 50 ng/cm^2. As shown in Figure 5, TFTs prepared with an areal density

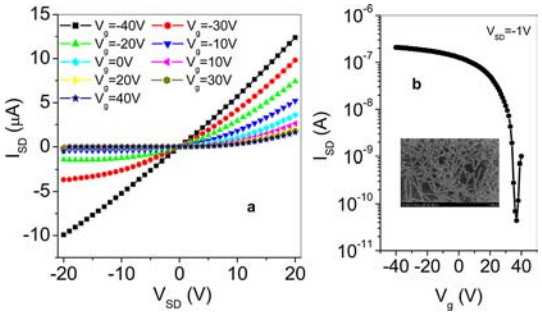

Figure 5. (a) Source-drain I–V curves and (b) transfer characteristics of a DWCNT TFT after covalent diazonium functionalization. Inset shows a SEM image of the DWCNT thin film.

of 35 ng/cm^2 DWCNTs possessed excellent transistor characteristics. Even after functionalization by $-C_6H_5COOH$ groups, this device still exhibited on/off ratio as high as 4000 when measured in water.

The high on/off ratio is more consistently achieved with low density CNT networks. The low density of the nanotube network is necessary to avoid percolation of metallic nanotubes, which would otherwise electrically short the device. The observed high on/off ratio suggests that the transport is dominated by the semiconducting nanotubes in the network since their conductivity can be effectively modulated by the gate (Figures 3 and 5). Although the tube–tube contacts may affect the mobility of the device, they do not dominate the on/off ratio and thus play a secondary role in the sensing mechanism, explaining why the sidewall functionalization dictates the sensor performance. Higher on/off ratio may be achieved if DWCNTs with semiconducting inner tubes can be separated further from those with metallic inner tubes, or by decreasing the areal density of the DWCNT network. However, low DWCNT density also leads to low source-drain current due to the smaller quantity of DWCNTs within the network. With our device structure, the source-drain current of DWCNT TFTs with an areal density of 35 ng/cm^2 can be lower than 1 μA at V_g = −40 V and V_{SD} = −1 V, as shown in Figure 4. Vice versa, increasing DWCNT areal density increases the drain current of TFTs, but also decreases the on/off ratio of the device due to the larger number of DWCNTs with metallic inner tubes within the percolated network. In order to obtain sensor devices with

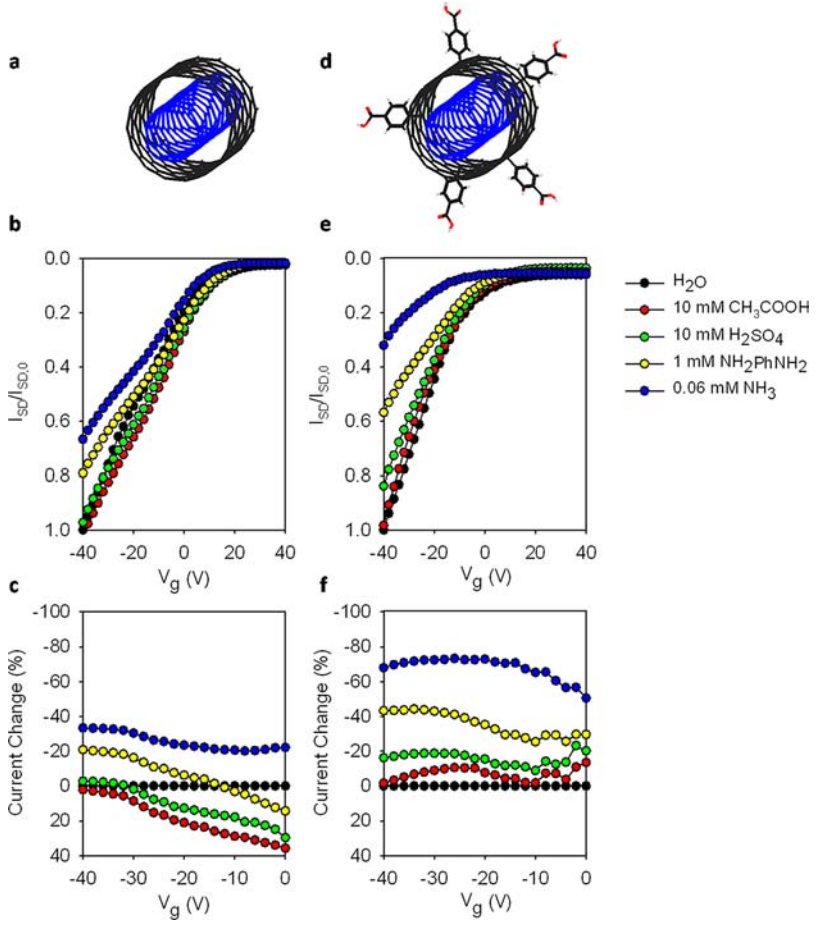

Figure 6. *f*-DWCNT TFTs show much higher chemical selectivity than that of pristine DWCNTs. A molecular model of (a) pristine and (d) functionalized DWCNT. Normalized response of (b) a pristine DWCNT TFT and (e) a $-C_6H_4COOH$ functionalized DWCNT TFT upon exposure to various analytes. The drain current is normalized relative to $I_{SD,0}$, the drain current measured at V_g= −40 V, V_{SD}= −1 V in H_2O. The corresponding current change ($\Delta I_{SD}/I_{SD,H2O}$ at each V_g) of (c) the pristine DWCNT TFT and (f) the *f*-DWCNT TFT upon exposure to various analytes.

dx.doi.org/10.1021/ja310844u | J. Am. Chem. Soc. 2013, 135, 2306–2312

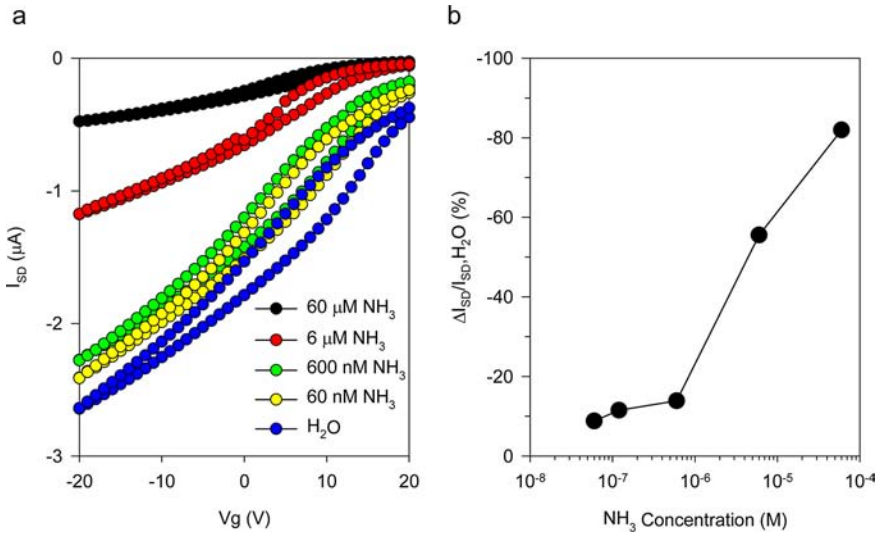

Figure 7. Sensitivity of *f*-DWCNT TFTs. (a) Transfer characteristics and (b) the normalized current change ($\Delta I_{SD}/I_{SD},H_2O$, at V_g = −20 V) of a *f*-DWCNT TFT as a function of NH_3 concentration.

desired on-current and reasonable on/off ratio, TFTs with a DWCNT areal density of 53 ng/cm^2 were chosen and used for the sensor platform.

To demonstrate the application of DWCNT TFTs for selective chemical detection, outer wall-functionalized and pristine DWCNT TFTs were tested in 0.06 mM NH_3, 1 mM NH_2PhNH_2, 10 mM CH_3COOH, and 10 mM H_2SO_4 aqueous solutions. Acids with higher concentrations than NH_3 were used in order to show the selective response of the sensors. Figure 6 compares the change in the transfer characteristics of DWCNT TFTs with and without functionalization upon exposure to analyte solutions. The normalized TFT response was plotted as a function of gate voltage. The device with -C_6H_4COOH functionalized DWCNT exhibited much higher response upon exposure to NH_3 and NH_2PhNH_2 compared to that of pristine DWCNT TFTs. For the pristine DWCNT TFT, a reduction of about 34% in drain current was observed when the device was exposed to 0.06 mM NH_3 solution, while 68%, or twice as much drain current reduction was observed for the functionalized DWCNT TFT. The normalized sensitivity (normalized drain-current change upon exposure to analytes, relative to water, per analyte concentration unit) of this device is as high as 1133% per mM NH_3. The sensitivity toward NH_2PhNH_2 was also improved by the −C_6H_4COOH functional groups. When the functionalized device was exposed to 1 mM NH_2PhNH_2 solution, we observed a 43% reduction in the drain current, versus the 22% with the pristine DWCNT TFTs. This nearly 2-fold increase in sensitivity can be attributed to the -C_6H_4COOH functional groups on outer walls of the heavily functionalized DWCNTs because of the acid−base interactions between the covalently attached carboxylic acids on the outer sidewall with the amine analytes. Because of this base-acid chemistry, the amine analyte induces a negative charge that reduces the hole density of the p-type carbon nanotube, giving rise to the observed selectivity over acids.

In addition, the normalized sensitivity (1133% per mM) of the functionalized DWCNT TFT upon exposure to 0.06 mM NH_3 was 6000 times higher than the sensitivity to 10 mM acetic acid (0.17% per mM), which demonstrates the chemical selectivity of this novel sensor device based on the chemical interactions between the terminal groups on the outer sidewall with analytes. The diversity of sensor responses observed upon exposure to different analytes shows the selectivity of the sensor device.

To further demonstrate the capability of covalently functionalized DWCNTs for low-concentration small molecule detection, a -C_6H_5COOH functionalized DWCNT TFT was tested in diluted NH_3 solutions varying from 60 nM to 60 μM. The change of transfer characteristics of this device upon exposure to successively increasing concentrations of NH_3 solution is shown in Figure 7a, with the transfer characteristics measured in nanopure water acting as the baseline. Time-dependent measurements confirm the devices exhibit reversible increase in ON-current upon introduction of NH_3 solutions and replacement with water (Figure S5 of the SI). Figure 7b summarizes the corresponding relative drain current response ($\Delta I_{SD}/I_{SD,H2O}$) of this DWCNT TFT as a function of NH_3 concentration. Drain current measured at V_g= −20 V and V_{SD}= −1 V was used as output signal. We note that a V_g of −20 V, instead of −40 V, is chosen here to prevent device damage during repetitive measurements and baseline shift due to gate bias stress effects. NH_3 was detected at concentrations as low as 60 nM in water, which is comparable to state-of-the-art TFT sensors based on SWCNTs.[11,31] This value may be further improved by optimizing device structure and utilizing external aid such as preconcentrators.

■ CONCLUSIONS

We proposed a double-wall materials concept to address the challenge of simultaneously attaining ultrahigh selectivity and sensitivity in electrical sensing based on carbon nanostructures. Proof-of-concept TFT devices based on covalently functionalized DWCNTs were fabricated and analyzed against SWCNT and MWCNT TFTs for the detection of different amines in aqueous solutions. We found that the covalently functionalized DWCNT TFTs yielded excellent transistor properties showing an on/off ratio as high as 4000. With carboxylic acid-functionalized outer walls, the devices displayed a sensitivity of 60 nM (or ∼1 ppb), while simultaneously displaying a chemical selectivity as high as 6000 toward a variety of amine containing analyte molecules over other small molecule analytes. This combined ultrahigh sensitivity and selectivity

was made possible by the unique double-wall structure of DWCNTs, which simultaneously enables high sensitivity of SWCNT TFTs and the desirable chemical selectivity by outer wall selective covalent modification. This double-wall device platform thus opens new opportunities for chemical and biological sensing where simultaneous sensitivity and selectivity are desirable for detecting trace analytes of interest within the typically complex chemical environments.

EXPERIMENTAL SECTION

Nanotube Dispersions. High-purity DWCNTs were separated from a CVD-grown sample (Unidym DW411UA) using density gradient ultracentrifugation (DGU).[23] The sorted DWCNTs have an average diameter of 0.86 and 1.61 nm for the inner and outer wall nanotubes, respectively. Purified arc-discharge MWCNTs (n-Tec) were dispersed in aqueous 0.25% sodium dodecyl sulfate. SWCNT solutions were prepared using a procedure derived from a previous publication.[32] Raw SWCNTs (10 mg, HiPco Lot R0513) were dispersed in a 25 mL of aqueous 1% sodium cholate solution (99.9% Sigma Aldrich) by tip-sonication (MISONIX ultrasonicator operated at a power level of 17 W) in a cooled (15 °C) stainless steel cup for 2 h. The nanotube dispersion was centrifuged at 64,700g for 2 h (Beckman Coulter Optima LE-80K; 70 Ti fixed angle rotor), after which the supernatant was collected. The concentrations of the SWCNT dispersions were adjusted with 1% sodium cholate/H_2O solution to a similar optical absorbance as that of the DWCNT solution (O.D. ≈ 0.032 @ 1000 nm).

Diazonium Salts Preparation. 4-Aminobenzoic acid (4.814 mmol, 99%, Sigma Aldrich) was added to 3 mL of nanopure water in a 10 mL round-bottom flask. An aqueous solution of tetrafluoroboric acid (2.68 mL, 48 wt.%, Sigma Aldrich) was then added and the mixture cooled in an ice bath. 670 mg of sodium nitrite (Sigma Aldrich, ≥97.0%) was dissolved in 2 mL of nanopure water and added dropwise to the mixture while stirring. The mixture was allowed to react for 15 min. The precipitated diazonium salt was collected and washed with ~200 mL of diethyl ether. The purified salt was dried under vacuum in the dark for 20 min. The salt was stored at 4 °C and was used within a week after synthesis.

Raman Spectroscopy. Raman spectra were collected on Horiba Jobin Yvon LabRAM Raman microscope (model ARAMIS) with excitation lines that included 532 and 633 nm.

UV–vis-NIR Absorption Spectroscopy. Optical absorption spectra were measured using a PerkinElmer Lambda 1050 UV–vis-NIR spectrophotometer equipped with a PMT and an InGaAs detector.

Device Fabrication. Heavily doped silicon wafers with 300 nm of thermally grown silicon dioxide were used as substrates for all the devices. Prior to the fabrication, the substrates were cleaned by rinsing sequentially with acetone, 2-propanol, ethanol, and water. Bottom-gate top-contact CNT TFTs were fabricated on carbon nanotube thin films that were prepared using a modified filtration method.[33] CNT solutions were filtered through 47 mm mixed cellulose ester (MCE) filter membranes and rinsed with water to remove surfactant. The resulting percolated CNT films along with the filter membranes were placed onto the substrate with the CNT films contacting with silicon oxide surfaces, compressed by applying force, and thermally annealed at 95 °C for one hour to provide the nanotube film with sufficient adhesion to the substrate. After heating and compression, the MCE filter membrane was dissolved using an acetone vapor bath and rinsed with fresh acetone and ethanol. Finally, Cr (10 nm) and Au (50 nm) electrodes were thermally evaporated through shadow masks. Channel length and width are 2.5 and 4.0 mm, respectively. For devices with surface functionalization, the CNT TFTs were immersed into 236 mg L^{-1} diazonium solution and slowly stirred for 24 h in the dark at room temperature, followed by copious rinsing in nanopure water.

Small Molecule Detection. For aqueous sensing measurements, a rectangular region was defined using electronic coating polymer (3 M Co. Novec, EGC-1700) to hold a liquid droplet on each CNT TFT. The polymer was used to protect the Au electrodes from direct contact with the liquid solution. Each sensor was tested sequentially in air, nanopure water, and analyte solutions. Electrical measurements in liquid were performed by placing a droplet (4 μL) of liquid in the designed region between the source-drain electrodes, with the entire channel immersed by the liquid. All DWCNT TFTs exhibited robust performance with stable drain currents in water. No obvious degradation of the CNT TFTs was observed during the measurements. Source-drain current–voltage (I_{SD}–V_{SD}) curves of the sensors in nanopure water were measured as the baseline for the devices. After the baselines were established, another droplet of analyte solution was added into the pool and I–V curves were measured over time. To recover the sensor devices, sensors were rinsed with copious amounts of nanopure water and then vacuum-dried for 24 h to remove water.

ASSOCIATED CONTENT

Supporting Information

SEM images and optical properties of nanotube networks. This material is available free of charge via the Internet at http://pubs.acs.org.

AUTHOR INFORMATION

Corresponding Author

yhw@umd.edu

Present Address

[#]School of Materials Science and Engineering, Tongji University, 4800 Caoan Road, Shanghai 201804, China.

Notes

The authors declare no competing financial interest.

ACKNOWLEDGMENTS

This work was partially supported by the University of Maryland, the National Science Foundation (CAREER CHE–1055514), and the Office of Naval Research (N000141110465). DWCNT purification was supported by the National Science Foundation (DMR-1006391 and DMR-1121262) and the Nanoelectronics Research Initiative (M.C.H.). A Natural Sciences and Engineering Research Council of Canada Postgraduate Scholarship is also acknowledged (A.A.G.).

REFERENCES

(1) Kong, J.; Franklin, N. R.; Zhou, C.; Chapline, M. G.; Peng, S.; Cho, K.; Dai, H. *Science* **2000**, *287*, 622.
(2) Chen, R. J.; Bangsaruntip, S.; Drouvalakis, K. A.; Kam, N. W. S.; Shim, M.; Li, Y.; Kim, W.; Utz, P. J.; Dai, H. *Proc. Nat. Acad. Sci. U.S.A.* **2003**, *100*, 4984.
(3) Star, A.; Tu, E.; Niemann, J.; Gabriel, J.-C. P.; Joiner, C. S.; Valcke, C. *Proc. Natl. Acad. Sci. U. S. A.* **2006**, *103*, 921.
(4) Sorgenfrei, S.; Chiu, C.-Y.; Gonzalez, R. L., Jr.; Yu, Y.-J.; Kim, P.; Nuckolls, C.; Shepard, K. L. *Nat. Nanotechnol.* **2011**, *6*, 126.
(5) Kim, T. H.; Lee, S. H.; Lee, J.; Song, H. S.; Oh, E. H.; Park, T. H.; Hong, S. *Adv. Mater.* **2009**, *21*, 91.
(6) Li, C.; Curreli, M.; Lin, H.; Lei, B.; Ishikawa, F. N.; Datar, R.; Cote, R. J.; Thompson, M. E.; Zhou, C. *J. Am. Chem. Soc.* **2005**, *127*, 12484.
(7) Ganzhorn, M.; Vijayaraghavan, A.; Dehm, S.; Hennrich, F.; Green, A. A.; Fichtner, M.; Voigt, A.; Rapp, M.; Von Löhneysen, H.; Hersam, M. C.; Kappes, M. M.; Krupke, R. *ACS Nano* **2011**, *5*, 1670.
(8) Cao, Q.; Rogers, J. A. *Adv. Mater.* **2009**, *21*, 29.
(9) Kim, T. H.; Lee, B. Y.; Jaworski, J.; Yokoyama, K.; Chung, W.-J.; Wang, E.; Hong, S.; Majumdar, A.; Lee, S.-W. *ACS Nano* **2011**, *5*, 2824.
(10) Forzani, E. S.; Li, X.; Zhang, P.; Tao, N.; Zhang, R.; Amlani, I.; Tsui, R.; Nagahara, L. A. *Small* **2006**, *2*, 1283.
(11) Roberts, M. E.; LeMieux, M. C.; Bao, Z. *ACS Nano* **2009**, *3*, 3287.

(12) Myung, S.; Solanki, A.; Kim, C.; Park, J.; Kim, K. S.; Lee, K.-B. *Adv. Mater.* **2011**, *23*, 2221.
(13) Myung, S.; Yin, P. T.; Kim, C.; Park, J.; Solanki, A.; Reyes, P. I.; Lu, Y.; Kim, K. S.; Lee, K.-B. *Adv. Mater.* **2012**, *24*, 6081.
(14) Martínez, M. T.; Tseng, Y.-C.; Ormategui, N.; Loinaz, I.; Eritja, R.; Bokor, J. *Nano Lett.* **2009**, *9*, 530.
(15) Pacios, M.; Martin-Fernandez, I.; Borrise, X.; del Valle, M.; Bartroli, J.; Lora-Tamayo, E.; Godignon, P.; Perez-Murano, F.; Esplandiu, M. J. *Nanoscale* **2012**, *4*, 5917.
(16) Wang, F.; Swager, T. M. *J. Am. Chem. Soc.* **2011**, *133*, 11181.
(17) Goldsmith, B. R.; Coroneus, J. G.; Khalap, V. R.; Kane, A. A.; Weiss, G. A.; Collins, P. G. *Science* **2007**, *315*, 77.
(18) Shen, C.; Brozena, A. H.; Wang, Y. *Nanoscale* **2011**, *3*, 503.
(19) Liu, K.; Wang, W.; Xu, Z.; Bai, X.; Wang, E.; Yao, Y.; Zhang, J.; Liu, Z. *J. Am. Chem. Soc.* **2009**, *131*, 62.
(20) Bouilly, D.; Cabana, J.; Meunier, F. o.; Desjardins-CarriÄre, M.; Lapointe, F. o. L.; Gagnon, P.; Larouche, F.; Adam, E.; Paillet, M.; Martel, R. *ACS Nano* **2011**, *5*, 4927.
(21) Endo, M.; Muramatsu, H.; Hayashi, T.; Kim, Y. A.; Terrones, M.; Dresselhaus, M. S. *Nature* **2005**, *433*, 476.
(22) Qi, H.; Qian, C.; Liu, J. *Nano Lett.* **2007**, *7*, 2417.
(23) Green, A. A.; Hersam, M. C. *Nat. Nanotechnol.* **2009**, *4*, 64.
(24) Green, A. A.; Hersam, M. C. *ACS Nano* **2011**, *5*, 1459.
(25) Brozena, A. H.; Moskowitz, J.; Shao, B.; Deng, S.; Liao, H.; Gaskell, K. J.; Wang, Y. *J. Am. Chem. Soc.* **2010**, *132*, 3932.
(26) Piao, Y.-M.; Chen, C.-F.; Green, A. A.; Kwon, H.-J.; Hersam, M. C.; Lee, C. S.; Schatz, G. C.; Wang, Y. *J. Phys. Chem. Lett.* **2011**, *2*, 1577.
(27) Kalbac, M.; Green, A. A.; Hersam, M. C.; Kavan, L. *ACS Nano* **2010**, *4*, 459.
(28) Kalbac, M.; Green, A. A.; Hersam, M. C.; Kavan, L. *Chem.—Eur. J.* **2011**, *17*, 9806.
(29) Nair, N.; Kim, W.-J.; Usrey, M. L.; Strano, M. S. *J. Am. Chem. Soc.* **2007**, *129*, 3946.
(30) Doyle, C. D.; Rocha, J.-D. R.; Weisman, R. B.; Tour, J. M. *J. Am. Chem. Soc.* **2008**, *130*, 6795.
(31) Peng, N.; Zhang, Q.; Chow, C. L.; Tan, O. K.; Marzari, N. *Nano Lett.* **2009**, *9*, 1626.
(32) O'Connell, M. J.; Bachilo, S. M.; Huffman, C. B.; Moore, V. C.; Strano, M. S.; Haroz, E. H.; Rialon, K. L.; Boul, P. J.; Noon, W. H.; Kittrell, C.; Ma, J.; Hauge, R. H.; Weisman, R. B.; Smalley, R. E. *Science* **2002**, *297*, 593.
(33) Wu, Z.; Chen, Z.; Du, X.; Logan, J. M.; Sippel, J.; Nikolou, M.; Kamaras, K.; Reynolds, J. R.; Tanner, D. B.; Hebard, A. F.; Rinzler, A. G. *Science* **2004**, *305*, 1273.